Hydration−Dehydration-Induced Reversible Ordering−Disordering Transition of the Molecular Arrangement on the Surface of KCP(Br) Single Crystals

Tatsuji Kawasaki,[†,‡] Lei Jiang,[†] Tomokazu Iyoda,[†,§] Toshinari Araki,[‡] Kazuhito Hashimoto,[†,||] and Akira Fujishima*[,†,||]

Kanagawa Academy of Science and Technology, 1583 Iiyama, Atsugi, Kanagawa 243-02, Japan, Tokyo Gas Co., Ltd., 7-7 Suehiro-cho, 1-Chome, Tsurumi-ku, Yokohama, Kanagawa 230, Japan, Department of Industrial Chemistry, Faculty of Engineering, Tokyo Metropolitan University, 1-1 Minami-Osawa, Hachioji, Tokyo 192-03, Japan, and Department of Applied Chemistry, Faculty of Engineering, University of Tokyo, Hongo, Bunkyo-ku, Tokyo 113, Japan

Received: September 12, 1997

Molecular-resolution images by atomic force microscopy (AFM) revealed a reversible ordering−disordering transition of molecular arrangements on the (010) face of a single crystal of potassium tetracyanoplatinate bromide (KCP(Br)) during dehydration and hydration treatments. The intracolumnar Pt−Pt distance along the *c*-axis in the dehydrated crystal lengthens by a factor of 30% with considerable disordering, and the rehydrated crystal shows well-ordered arrangement like the as-grown crystal, while the intercolumnar structure along the orthogonal direction is not varied. Large-scale AFM images showed that the monolayer terraces reversibly slide in the *c*-axis direction during the dehydration−hydration treatments, reflecting the molecular dislocation along the *c*-axis. This surface structural change is quite consistent with well-known dehydration effects in KCP(Br) crystals, i.e., the lattice disordering and the decreasing conductivity.

Introduction

The mixed-valence quasi-one-dimensional (1-D) conducting platinum compound $K_2Pt[CN]_4Br_{0.3}\cdot 3.2H_2O$ (KCP(Br)) (Figure 1) has attracted much interest because of its anisotropic electrical conductivities, optical dichroism, and highly symmetric simple structure, which is adaptable to the theory of one-dimensional metals.[1−4] The high conductivity originates from the short intracolumnar Pt−Pt distance, leading to electron delocalization along the column. The conduction properties and associated phenomena should be significantly influenced by arrangements of the tetracyanoplatinate unit, interstitial ions, and crystal water. A reversible change, by a factor on the order of 4, in conductivity between the dehydrated and hydrated crystals has been reported by Drosdziok and co-workers.[5] These results suggest that water molecules in the crystal lattice may play a very important role in the electronic states of the conducting column. Furthermore, Butler pointed out that the decreasing conductivity with dehydration may result from changes in the local electric field inside the crystal.[6] Both X-ray and neutron diffuse-scattering experiments[7] have been conducted to observe Peierl's distortions and charge density wave displacements in the crystals. The X-ray diffraction study suggested a statistical disordering of the molecular arrangement in the bulk of the dehydrated crystal.[8,9] However, no direct evidence of a molecular-level structural change has been reported. Atomic force microscopy is a useful tool to study local molecular arrangements, compared with the diffraction technique. In particular, any change in the surface molecular arrangements must have an effect on the electric conduction properties in the KCP(Br) crystal, which is precisely our motivation for carrying out the present study. Herein, we report a dehydration−hydration-induced reversible molecular rearrangements on the (010) face of the KCP(Br) crystals using AFM study under a controlled humidity atmosphere.

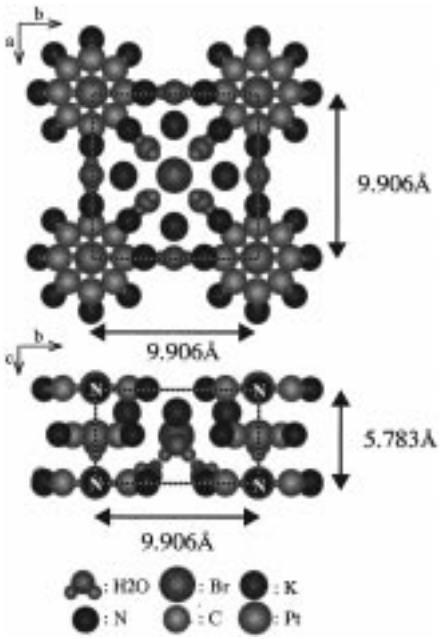

Figure 1. Structure of $K_2Pt[CN]_4Br_{0.3}\cdot 3.2H_2O$, abbreviated KCP(Br). (a) KCP(Br) consists of staggered tetracyanoplatinate units that are tilted 45° with respect to the neighboring units. (b) The KCP(Br) crystal belongs to the monoclinic space group *P*4*mm* and has unit cell dimensions as follows: $a = b = 9.906$ Å and $c = 5.783$ Å.

Experiment

The KCP(Br) single crystals were prepared by the electrochemical method described previously.[10] The AFM measure-

[†] Kanagawa Academy of Science and Technology.
[‡] Tokyo Gas Co., Ltd.
[§] Tokyo Metropolitan University.
[||] University of Tokyo.

S1089-5647(97)03001-0 CCC: $15.00
Published on Web 02/20/1998

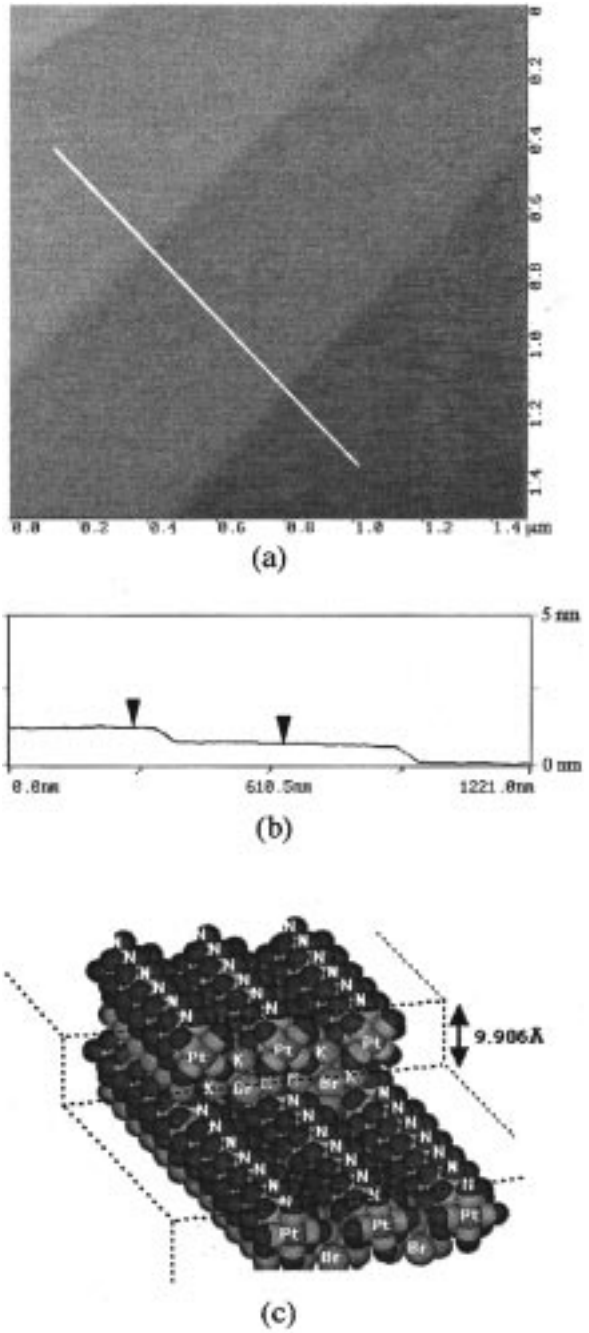

Figure 2. (a) Large-scale AFM image (1.5 μm × 1.5 μm) of the side surface of a freshly prepared KCP(Br) crystal in the constant height mode. (b) Cross section showing that each step height is 10.5 ± 0.6 Å. (c) The molecular model of the monolayer step.

ments were carried out using an SPA300 AFM (Seiko Instruments) in a sealed chamber in which the relative humidity was adjusted by flushing with either dry or humid N_2 gas, using Si_3N_4-coated cantilevers and a 20 μm piezoelectric tube scanner. As-grown single crystals were mounted on the stage with the side of the needle crystal, i.e., the (010) surface, facing up. The AFM measurements were carried out in both contact and noncontact modes. Before every contact mode measurement (for molecular resolution), the AFM system was calibrated by imaging a freshly cleaved mica surface. All of the molecular resolution images were low-pass-filtered (1 kHz) to enhance the features of the surface structures. The images were thoroughly checked to ensure that the structures were real and consistent by changing scan directions and magnifications.

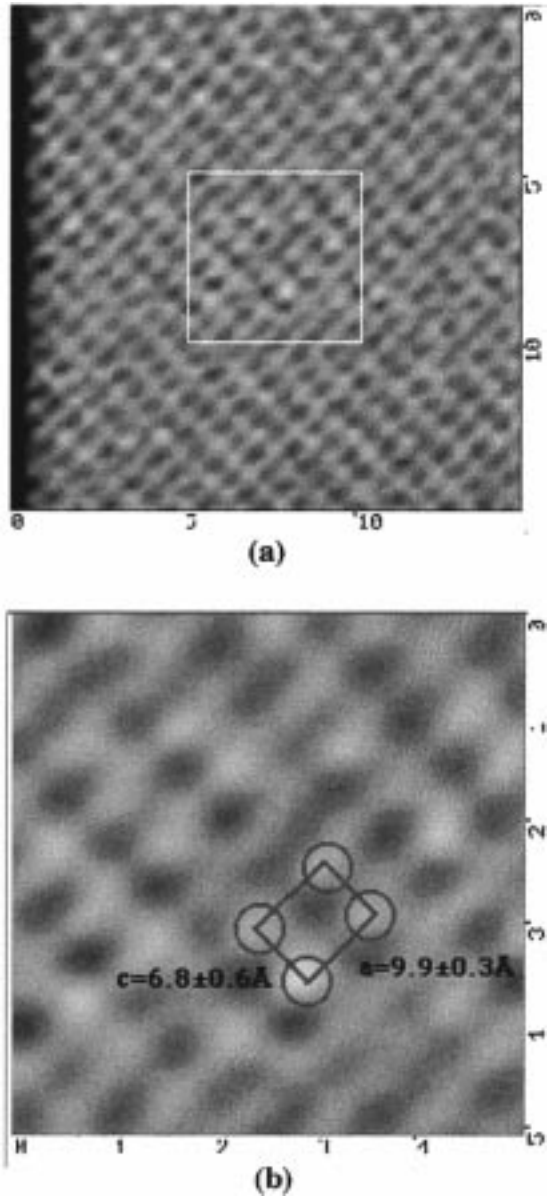

Figure 3. (a) Molecular resolution AFM images of the side surface of KCP(Br) before dehydration. Image size is 15 nm × 15 nm. (b) Magnified image (5 nm × 5 nm) of image a.

Results and Discussions

Figure 2a shows a large-scale contact-mode AFM image of the side surface of a freshly prepared KCP(Br) crystal. Terraces with several steps were observed on the surface. The cross section of the image in Figure 2b indicates that each step height is 10.5 ± 0.6 Å, consistent with the crystallographic parameter for the *a*- and *b*-axes (9.906 Å). Therefore, the observed face is assigned to the (010) face, with atomically flat terraces and monolayer steps, as shown in Figure 2c. The surfaces of these terraces were flat enough to acquire molecular-resolution images.

Figure 3a shows one of the molecular AFM images of the side surface of a freshly prepared KCP(Br) ($K_2Pt(CN)_4Br_{0.3}\cdot 3.2H_2O$)[11] crystal in the constant height mode. Parallel long columnar structures consisting of periodic bright spots were observed in the image. The columns are aligned along the long axis of the crystal mounted on the stage, so that the direction can be assigned to [001]. Figure 3b shows a magnified image of Figure 3a. Four neighboring bright spots exhibit a rectangular arrangement, with edges of 9.9 ± 0.3 and 6.8 ± 0.6 Å. We

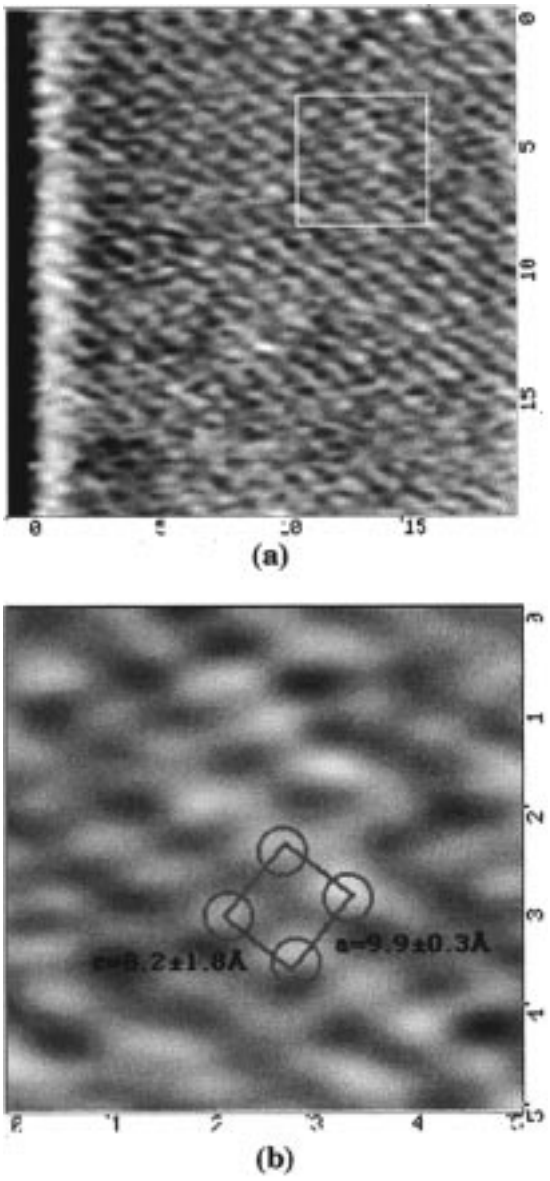

Figure 4. (a) Molecular resolution AFM images of the side surface of dried KCP(Br). Image size is 20 nm × 20 nm. (b) Magnified image (5 nm × 5 nm) of image a.

identified the individual spots in this image by referring to the space-filling model (Figure 1) constructed from the X-ray diffraction data.[12] The N atoms denoted in Figure 1 are the most protruding nitrogen (N) atoms of the cyanide ligands of the (010) face and correspond to the arrangement of the bright spots on the (010) surface in Figure 3b. We can conclude that this molecular-level topography reflects the columnar structure of the staggered tetracyanoplatinate units on the (010) face. On the other hand, the dehydrated crystal ($K_2Pt(CN)_4Br_{0.3}\cdot 0.5H_2O$)[13] was prepared by keeping the crystal in vacuo for 2 days. Figure 4a shows an AFM image of the side surface of the dehydrated KCP(Br) crystal under the same operating conditions. Obviously, the molecular arrangement appears disordered. Figure 4b shows a magnified image of Figure 4a. Note that the Pt−Pt distance along the column is 8.2 ± 1.8 Å, which is larger than that of the as-grown crystal, while the intercolumnar Pt−Pt distance is not changed (9.9 ± 0.3 Å). Moreover, while the elliptical spots appear in a regular pattern in the fresh hydrated crystal, the spot arrangement becomes disordered in the dehydrated crystal. Figure 5 shows a distribution of the intracolumnar Pt−Pt distances measured from the two AFM

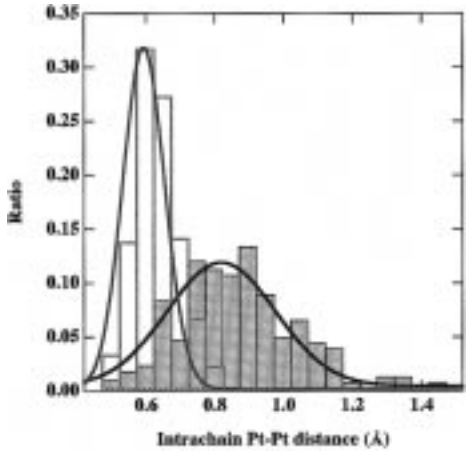

Figure 5. Distribution of lattice parameters of both the fresh (unshaded) and dehydrated (shaded) crystals of KCP(Br). The histogram of the lattice parameters of the freshly prepared crystal included 296 samplings. The histogram in the case of the dehydrated crystal included 380 samplings.

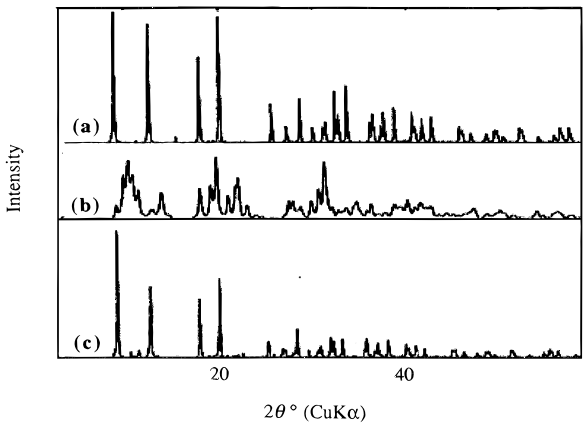

Figure 6. Powder X-ray diffraction patterns of KCP(Br): (a) as-grown hydrated crystal; (b) crystal after dehydration; and (c) crystal after rehydration.

images. This histogram clearly shows that the Pt−Pt distances in the dehydrated crystal are distributed more widely than those in the hydrated crystal and that the average Pt−Pt distance becomes longer by a factor of 30%. The powder X-ray diffraction analysis, as shown in Figure 6, indicated that the lattice parameters of the hydrated crystal are $a = b = 9.906$ Å and $c = 5.783$ Å, in agreement with published results.[12] However, the dehydrated crystal had extremely poor crystallinity, exhibiting only some of the strongest peaks of the fresh crystal (Figure 6b). After the crystal was stored under high humidity conditions for 30 min, the diffraction pattern of the dehydrated crystal reverted back to that of the as-grown crystal (Figure 6c). It should be noted that good reversibility of these disordering−ordering structural changes was observed as a result of dehydration and rehydration treatments, respectively. Dehydration may induce a weak interlayer interaction, which might allow individual monolayers to easily slide with 30% expansion along the *c*-axis, i.e., an anisotropic molecular rearrangement. These observations may also lead us to expect a macroscopic morphological change on the surface of the crystal.

Figure 7a shows a large-scale noncontact-mode AFM image of the side surface of a freshly prepared KCP(Br) crystal. Atomically flat terraces with several monolayer steps were observed on the surface. Figure 7b shows an AFM image of the same sample after flushing with dry N_2 gas in the sealed sample chamber for 30 min. The smooth step edges become

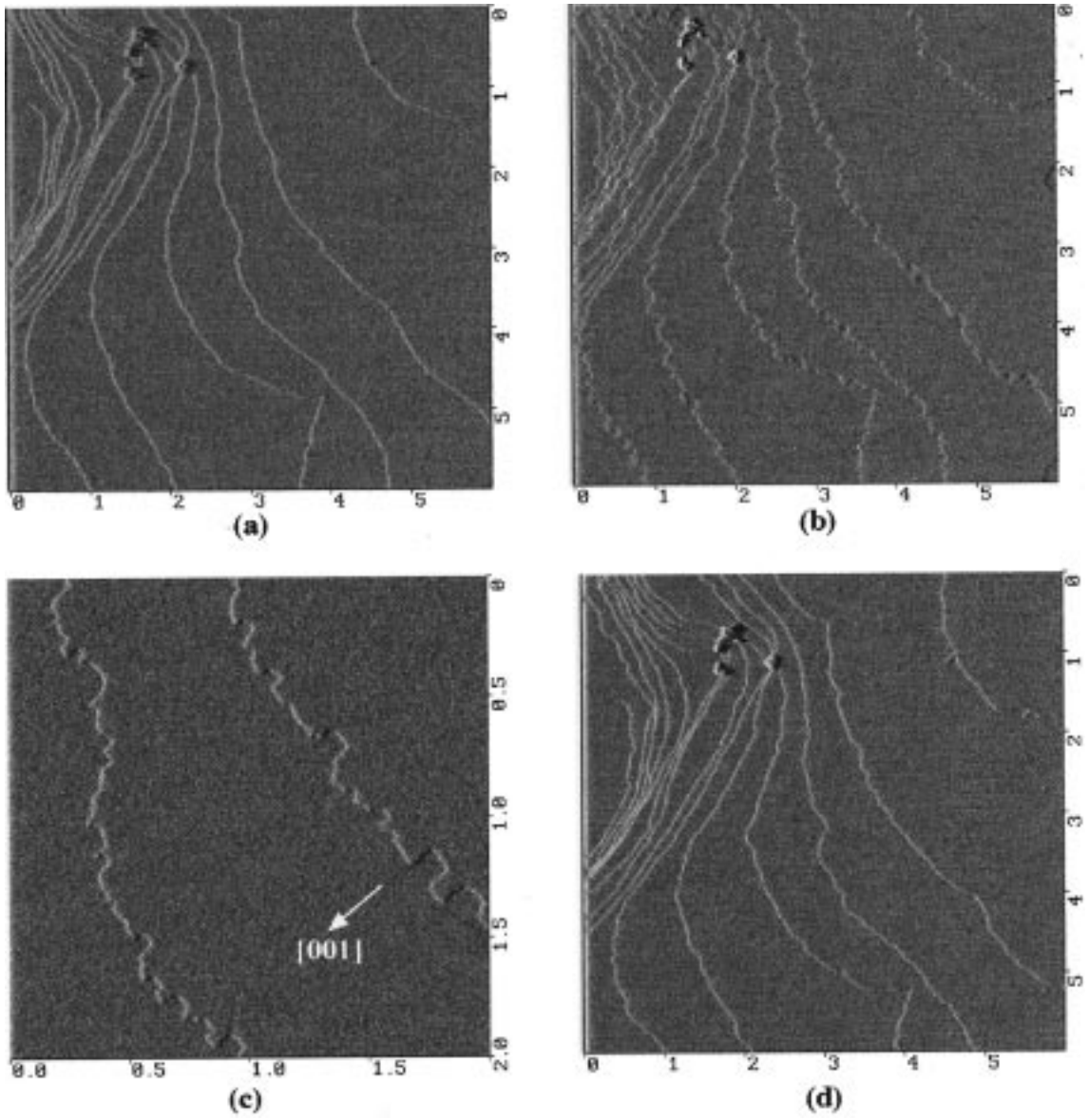

Figure 7. (a) Large-scale AFM image (6 μm × 6 μm) of the side surface of a freshly prepared KCP(Br) in noncontact mode. (b) AFM image that was obtained on the same scanning area after dehydration in a sealed chamber in which the relative humidity was adjusted by flushing with dry or humid N_2 gas. (c) Zoomed-in image (2 μm × 2 μm) of b showing rectangular edge structure. (d) AFM image that was obtained on the same scanning area after hydration in a sealed chamber in which the relative humidity was adjusted by flushing with humid N_2 gas.

irregular, while the height of each step was essentially unchanged before and after dehydration. Moreover, it was found that the step edges extend in the [001] direction, which is the direction of the conducting columns. Figure 7c shows a zoomed-in image of Figure 7b in which there are several rectangular hollows with [001] and [100] edges arranged parallel to the *c*-axis. This phenomenon results from an anisotropic molecular rearrangement on the microscopic scale and also suggests that different degrees of dehydration may occur in various layer edge areas. Furthermore, to our surprise, the irregular edge reverted back to the original smooth edge, after flushing with humid N_2 in a sealed chamber for 1 h (Figure 7d). Although molecular rearrangements occur during these dehydration and hydration processes, the molecules appear to always retain a layered structure. This implies that the intracolumnar molecular interactions between tetracyanoplatinate units should be much stronger than the intercolumnar interactions, even during hydration and dehydration processes.

All of these results demonstrate a direct observation of a reversible dehydration−hydration process on the surfaces of KCP(Br) crystals. The disordering transition of the molecular arrangement on the (010) face of KCP(Br) during dehydration may be induced by a change in the electrostatic stabilization of the tetracyanoplatinate units, interstitial K^+ ions, and Br^- ions resulting from the loss of crystal water molecules. Crystals of the starting material, potassium tetracyanoplatinate(II), have a disk-stacking structure of square-planar tetracyanoplatinate units, with a 3.478 Å Pt−Pt distance and a 15.7° torsional angle between the neighboring units.[2] KCP(Br) has partially oxidized tetracyanoplatinate units, in other words, a mixed-valence state consisting of Pt^{II} and Pt^{IV}, since all of the Pt atoms are crystallographically identical.[14,15] The mixed-valence conducting column consists of staggered tetracyanoplatinate units with a 45° torsional angle. This torsional angle minimizes steric hindrance between the cyanide ligands on the neighboring tetracyanoplatinate units. The crystal water molecules reside at positions between the bromide ions and platinum ions, as shown in Figure 1. The water molecules inside the crystal may play a significant role in the molecular arrangement in the crystal through hydrogen bonding and as a polar medium for Coulombic

interactions. The column may become stabilized through rotation of $[Pt(CN)^4]^{n-}$ units so as to maintain electrostatic force balance after dehydration, just as in crystals of the starting material, potassium tetracyanoplatinate(II). Thus, the transition of the mixed-valence state to the localized state, in which the valence states of Pt^{II} and Pt^{IV} are distinguishable, results in the disordered intracolumnar arrangement. In addition, these water molecules contribute to the interactions between interlayers. The dehydration may reduce interlayer interactions, so that layer sliding can take place.

In summary, hydration−dehydration-induced reversible morphological changes due to the molecular rearrangement were directly observed with AFM. We confirmed that the decreasing conductivity of KCP(Br) single crystals during dehydration should result from the molecular rearrangement process, in which breaks in the electron transport channel may occur along the column direction due to expansion and the irregularity of intracolumnar Pt−Pt distances.

References and Notes

(1) Miller, J. S.; Epstein, A. J. *Prog. Inorg. Chem.* **1976**, *20*, 1.
(2) Keller, H. J. In *Extended Linear Chain Compounds*; Miller, J. S., Ed.; Plenum, New York, 1982; Vol. 1.
(3) Shchegolev, I. F. *Phys. Status Solidi A* **1972**, *12*, 9.
(4) Rice, M. J. *Phys. Bull.* **1975**, *26*, 493.
(5) Drosdziok, S.; Engbrodt, M. *Phys. Status Solidi B* **1975**, *72*, 739.
(6) Bulter, M. A.; Guggenheim, H. J. *Phys. Rev. B* **1974**, *10*, 1778.
(7) Carneiro, K.; Shirane, G.; Werner, S. A.; Kaiser, S. *Phys. Rev. B* **1976**, *13*, 4258.
(8) Drosdziok, S.; Engbrodt, M. *Solid State Commun.* **1975**, *17*, 1339.
(9) Cahen, D. *Solid State Commun.* **1973**, *12*, 1091.
(10) Kawasaki, T.; Jiang, L.; Iyoda, T.; Araki, T.; Tryk, D. A.; Hashimoto, K.; Fujishima, A. *Chem. Lett.* **1995**, *10*, 879. Kawasaki, T.; Jiang, L.; Iyoda, T.; Araki, T.; Hashimoto, K.; Fujishima, A. *J. Phys. Chem. B* **1997**, *101*, 2723.
(11) Elemental analysis of the crystal was as follows: C, 10.4%; N, 12.1%; Br, 5.3%; K, 15.5%; Pt, 41.9%; and H_2O, 12.7%.
(12) Peters, C.; Eagen, C. F. *Inorg. Chem.* **1976**, *15*, 782.
(13) Elemental analysis of the crystal was as follows: C, 11.9%; N, 14.1%; Br, 6.1%; K, 18.2%; Pt, 48.2%; and H_2O, 2.0%.
(14) Krogmann, K. *Angew. Chem., Int. Ed.* **1969**, *8*, 35.
(15) Zeller, H. R.; Beck, A. J. *J. Phys. Chem. Solids* **1974**, *35*, 77.